Table 2 Mean Distance from the Probes to the Poly(A) Tail Positions of Genes Showing Presence Solely in the UFT or Methacarn-Fixed PET[a]

aRNA Sample	UFT, 1× amplified	Methacarn-Fixed PET, 2× amplified
Mean distance from the 5′ end of the poly(A) tail (bp)		
No. of genes examined[b]	6	5
3′ end of the 5′ most probe	847	318[c]
3′ end of the 3′ most probe	569	97[c]

aRNA, antisense RNA; UFT, unfixed frozen tissue; PET, paraffin-embedded tissue.

[a] Genes obtained from microarray data in Table 1 were examined.

[b] All genes with sequence information for the 3′-untranslated region were examined.

[c] Significantly different from the unfixed frozen samples ($p < 0.01$).

ferences for male- or female-biased expression were found for 21% and 6% of all present genes, respectively (≥2-fold; Table 3). On EB-treatment, females demonstrated a greater number of genes with expression change. In males, up-regulation by EB was found for only 25 genes, all of them within 2- to 5-fold, and no genes showed down-regulation. In females, up-regulation was detected for a total of 586 genes after EB-treatment (≥2-fold), with 52 genes exhibiting ≥5-fold increase. When compared with up-regulated genes, down-regulated examples were fewer in number in females, with a total of 187 genes showing ≤1/2-fold down-regulation when compared with the vehicle control level. Among them, 33 genes showed ≤1/5-fold down-regulation when compared with vehicle controls. Relatively small numbers of genes showed altered expression on FA-treatment in both sexes. In males, only two and three genes showed up- and down-regulation, respectively (2- to 5-fold change), and in females, three and 22, all of them exhibiting 2- to 5-fold change, except for one gene with ≤1/5-fold up- and down-regulation, respectively.

Among genes showing male-biased expression (≥2-fold difference; 740 genes in total), 59% of them exhibited up-regulation on EB-treatment in females (≥2-fold; 437 genes in total), one of them also exhibiting up-regulation by FA in males (as shown in Fig. 4). One example alone showed down-regulation by FA in males. On the other hand, among genes showing female-biased expression (≥2-fold difference; 203 genes in total), 55% of them exhibited down-regulation by EB in females (≤1/2-fold; 111 genes in total). Among them, a total of 10 genes also showed altered expression by FA; nine genes down-regulated in females and one gene up-regulated in males. On the other hand, five female-predominant genes exhibited up-regulation by EB in males, four of them also showing down-regulation by EB in females, with one gene each further showing down-regulation in females and up-regulation in males by FA-treatment.

When genes that demonstrated changed expression levels in both sexes by the chemical treatments were examined, four genes encoding the LINE retrotransposable element 3, L1Rn B6 repetitive DNA element, ADP-ribosyltransferase (adprt) 1, and NonO/p54nrb homolog, exhibited up-regulation in males and down-regulation in females by EB-treatment and also female-biased expression (Table 4). Expression levels for genes showing male-biased expression were not affected by EB. FA-treatment did not alter the expression level of any gene involving both sexes.

Table 5 shows the list of genes showing altered expression in the MPOA of either sex common to both chemicals. Among the total of 15, 12 showed down-regulation in females common to EB and FA, eight of them exhibiting female-biased expression, i.e., for protein tyrosine phosphatase, receptor type, F (*PTPRF*); DAP-like kinase (*dlk*); glutamate receptor, kainate receptor subunit (KA1); dyskeratosis congenita 1 (*dyskerin*); L1Rn B6 repetitive DNA element; *MAP2*; expressed sequence tag (EST), similar to the mouse estrogen-responsive finger protein (*efp*); and glutamate receptor, ionotropic, AMPA subtype (GluR1).

Table 3 Number of Genes Showing Sex Differences in Basal Expression as well as Alteration After EB or FA Treatment in the Neonatal MPOA ($p < 0.05$)

Difference/Change (× fold)	2–5	≥5
Sex difference		
Males > females	676	64
Females > males	176	27
Altered by EB		
Males		
Up-regulated	25	0
Down-regulated	0	0
Females		
Up-regulated	534	52
Down-regulated	154	33
Altered by FA		
Males		
Up-regulated	2	0
Down-regulated	3	0
Females		
Up-regulated	3	0
Down-regulated	22	0

EB, estradiol benzoate; FA, flutamide; MPOA, medial preoptic area.

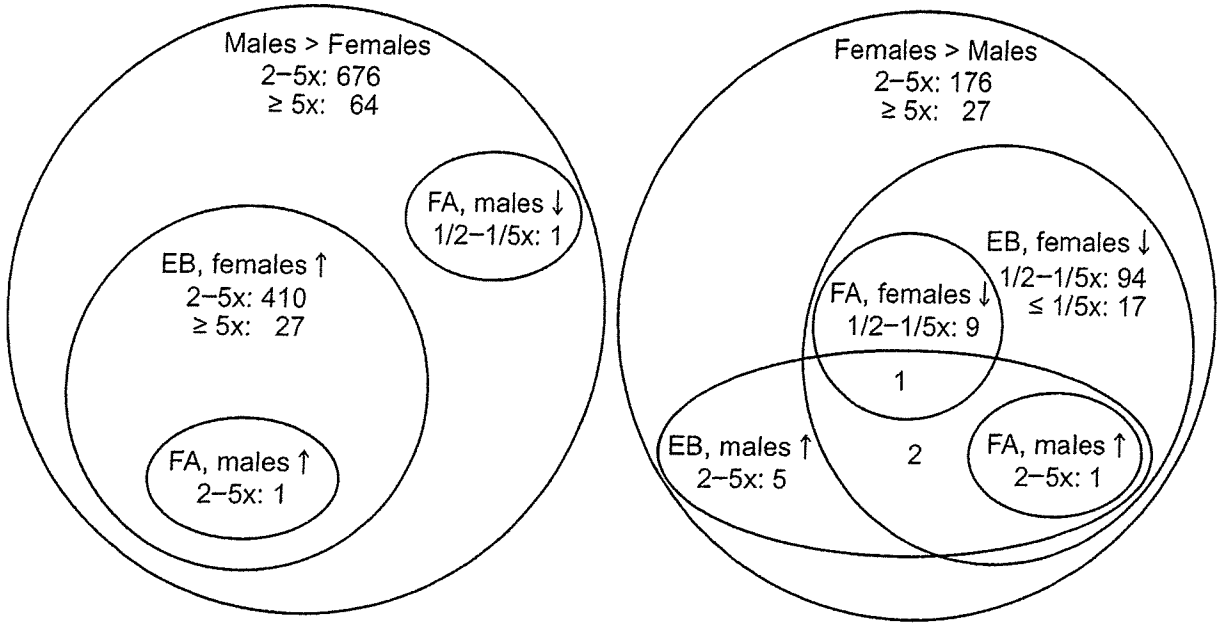

Figure 4 Distribution of gene populations showing altered expression with EB and/or FA-treatment among those showing sex differences in expression in the neonatal MPOA.

Interestingly, two subtypes of glutamate receptors, KA1 and GluR1, exhibited this particular expression pattern, the former being detected with two different probe sets (accession nos. U08257 and X59996). Without showing sex differences in the basal expression, expression of five genes were influenced by EB and FA, the following four exhibiting down-regulation in females with both chemicals: myeloid/lymphoid or mixed-lineage leukemia (trithorax (drosophila) homolog); translocated to, 3; cyclin D1; serine/threonine kinase 25; and neurotrimin. On the other hand, one EST (accession no. AI639097) showed up-regulation by EB and down-regulation by FA in females. Among the genes listed in Table 5, up-regulated examples were rather few and the magnitude of up-regulation was within 2- to 3-fold. In addition to the altered expression involving both sexes after EB treatment (see above), two genes showed altered expression with FA, i.e., down-regulation of the L1Rn B6 repetitive DNA element in females, and up-regulation of the LINE retrotransposable element 3 in males. Among those showing male-biased expression, there was only one with altered expression due to both EB and FA. MT1a transcripts showed up-regulation by EB in females and also by FA in males.

Fig. 5 shows mRNA expression data for two genes by real-time RT-PCR regarding sex differences in the neonatal MPOAs observed with microarrays. Both thymosin $\beta 4$ and Gαi2 mRNAs exhibited strong male-biased expression at PND 2, with 8.9- and 7.1-fold higher levels than in females. Real-time RT-PCR results confirmed this sex difference.

Immunoreactivity of Protein Signals

Fig. 6 shows representative figures for immunohistochemical demonstration of protein signals in the MPOA with the anatomical location indicated in

Table 4 List of Genes Showing Altered Expression in the MPOA of Both Sexes by EB-Treatment (≥2-fold, $p < 0.05$)

Accession No.	Gene	Sex Difference (× fold)	Altered by EB (× fold *vs.* control) M	F
M13100	LINE retrotransposable element 3	M<F (2.9)	2.1	0.5
X07686	L1Rn B6 repetitive DNA element	M<F (3.8)	2.0	0.4
AA964849	ADP-ribosyltransferase (adprt) 1	M<F (3.3)	2.2	0.3
AF036335	NonO/p54nrb homolog	M<F (5.5)	3.2	<0.1

MPOA, medial preoptic area; EB, estradiol benzoate; FA, flutamide; M, males; F, females; EST, expressed sequence tag.

Table 5 List of Genes Showing Altered Expression in the MPOA Common to EB and FA (≥2-fold, $p < 0.05$)

Accession No.	Gene	Sex Difference (× fold)	Altered by EB (× fold *vs.* control)		Altered by FA (× fold *vs.* control)	
			M	F	M	F
M13100	LINE retrotransposable element 3	M<F (2.9)	2.1	0.5	2.2	–
U87960	Protein tyrosine phosphatase, receptor type, F (PTPRF); leukocyte common antigen receptor (LAR)	M<F (11.8)	–	0.1	–	0.4
AJ006971	DAP-like kinase (dlk)	M<F (6.4)	–	0.3	–	0.3
U08257 (X59996)	Glutamate receptor, ionotropic, kainite 4 (Grik4); Kainate receptor subunit (KA1)	M<F (5.8) (M<F (5.4))	– (–)	0.3 (0.2)	– (–)	0.5 (0.5)
AA892562	Dyskeratosis congenita 1, dyskerin (dkc1)	M<F (4.0)	–	0.4	–	0.4
X07686	L1Rn B6 repetitive DNA element	M<F (3.8)	2.0	0.4	–	0.2
X53455	Microtubule-associated protein 2 (MAP2)	M<F (3.5)	–	0.1	–	0.3
AA859593	EST, similar to mouse estrogen-responsive finger protein (efp)	M<F (3.4)	–	0.3	–	0.5
X17184	Glutamate receptor, ionotropic, AMPA subtype, GluR1	M<F (3.1)	–	0.3	–	0.5
AJ006295	Myeloid/lymphoid or mixed-lineage leukemia (trithorax (Drosophila) homolog); translocated to, 3 (mllt3); AF-9	–	–	0.4	–	0.5
AI231257	Cyclin D1	–	–	0.4	–	0.5
AA799791	Serine/threonine kinase 25 (STE20 homolog, yeast) (stk25)	–	–	0.4	–	0.4
U16845	Neurotrimin	–	–	0.5	–	0.5
AI639097	EST	–	–	2.2	–	0.5
AI176456	Metallothionein (MT1a)	M>F (2.8)	–	2.9	2.3	–

MPOA, medial preoptic area; EB, estradiol benzoate; FA, flutamide; M, males; F, females; EST, expressed sequence tag.

Figure 1. In the hypothalamus at PND 2, nuclear immunoreactivity of PARP, the protein product of the *adprt* gene (Skaper, 2003), was observed in the ventricular ependymal and subependymal cells around the third ventricle. On quantitative measurement of nuclear immunoreactivity at the SDN region, cases with higher grades of distribution were more frequent in female controls when compared with the males [Figs. 6(A,B) and 7]. EB-treatment increased and decreased the positive cell distribution in males and females, respectively [Figs. 6(C) and 7]. GluR1 immunoreactivity was observed in the cytoplasm and dendritic processes of neuronal cells, its staining intensity being mostly weak in the MPOAs, even in the positive cases, when compared with the other brain areas, such as the hippocampus, cerebral cortex, and striatum [Fig. 6(D)]. In the MPOAs of male controls, two out of four cases showed only minimal intensity of GluR1-immunoreactivity, and the other two showed negative results [Fig. 6(D), Table 6]. Although the intensity was minimal to slight, all control females showed positive immunoreactivity in their MPOAs [Fig. 6(E)]. EB-treatment did not alter the intensity in either sex [female: Fig. 6(F)]. With regard to GluR5, very faint immunoreactivity was observed in the dendritic processes in the striatum and bed nucleus, but staining was lacking in the MPOAs of both sexes, even with the EB treatment

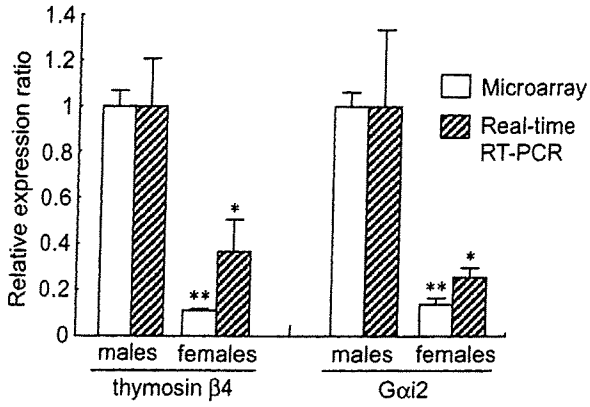

Figure 5 Confirmation of microarray data by real-time RT-PCR in the neonatal MPOA. Sex differences in the mRNA expression of thymosin $\beta 4$ and $G\alpha i2$ were analyzed. Significantly different from the male value in each detection system ($^*p < 0.05$, $^{**}p < 0.01$).

(Table 6). GluR6/7-immunoreactivity was observed in the cytoplasm of both neuronal and glial cells of the whole brain area, but there was no obvious change in terms of the distribution and intensity in the MPOAs, irrespective of the sex or EB treatment (Table 6). MAP2 immunoreactivity was observed in the whole dendritic processes with a fibrillary expression pattern, but there was no obvious change in terms of the distribution and intensity in the MPOAs, irrespective of the sex or EB treatment (Table 6). Strong cytoplasmic immunoreactivity of MT-1/2 was observed in the astrocytes located in the deep cortex and white matter of the cerebrum, hippocampal white matter, and striatum [Fig. 6(G)]. In other brain areas, MT-1/2-immunoreactivity was rather weak and sparse, and both nuclear and cytoplasmic. In the MPOAs, nuclear immunoreactivity predominated over cytoplasmic staining. On quantitative measurement of the nuclear immunoreactivity, the positive cell ratio was higher in males than in females, with increase in the latter on EB treatment [Figs. 6(G–I) and 7].

DISCUSSION

In the present validation study to establish a region-specific microarray analysis method using PET samples in combination with methacarn fixation, we found that gene expression profiles were very similar between 2×-amplified aRNAs from UFT and methacarn-fixed PET, and the deviation in expression data with the second-round amplification from the 1×-amplified aRNAs of UFT was mostly due to the preferential amplification of the 3′-terminal portion, irrespective of the tissue status. These results strongly indicate that methacarn fixation and subsequent paraffin embedding do not affect the expression fidelity in microarray analyses. Although it is still necessary to improve expression fidelity with second-round amplification, the results suggest an advantage of methacarn in combination with paraffin embedding for global gene expression analysis of microdissected cellular regions. It should be stressed that paraffin embedding is essential for preparation of serial sections necessary for microdissection of anatomically defined tissue areas.

Although the sex difference in the incidence of apoptosis in the SDN region that is believed to be re-

Figure 6 Immunoexpression patterns for PARP (panels A-C), GluR1 (panels D-F), and MT-1/2 (panels G-I), in the neonatal rat MPOA at PND 2. A. Note scattered PARP-immunoreactive nuclei (arrowheads) in paraventricular cells of a control male. The inset shows a high-power view of the nuclear weak immunoreactivity in the same area. B. Distribution of PARP-weakly immunoreactive cell nuclei in a control female. Note accumulation of positive cells in the SDN region (arrow). C. Lack of PARP-immunoreactive cells in most paraventricular and SDN regions in an EB-treated female. D. Very weak, mostly negative GluR1-immunoreactivity in the cytoplasmic processes of neurons in a control male. The inset shows strong immunoreactivity in the cytoplasm and dendritic processes of neuronal cells of the cerebral cortex of the same brain section. E. Slight intensity of GluR1-immunoreactivity in cytoplasmic processes of neurons in a control female. The inset shows a high-power view of the immunoreactivity in cytoplasmic processes of the same area. F. Minimal degree of GluR1-immunoreactivity in an EB-treated female. G. Diffuse immunoexpression of MT-1/2 in a control male. The expression pattern is mostly nuclear, and both astrocytic (arrowheads) and neuronal (arrows) populations as well as ependymal cells (*) show apparent immunoreactivity. The inset shows strong expression in cytoplasmic processes of astrocytes in the deep cerebral cortex of the same brain section. H. Scattered weak nuclear immunoreactivity of MT-1/2 in a control female. I. Diffuse nuclear and scattered cytoplasmic distribution of immunoreactive cells in an EB-treated female. The inset shows a high power view of both nuclear and cytoplasmic immunoreactivity in the same area. Bar = 50 μm, including insets.

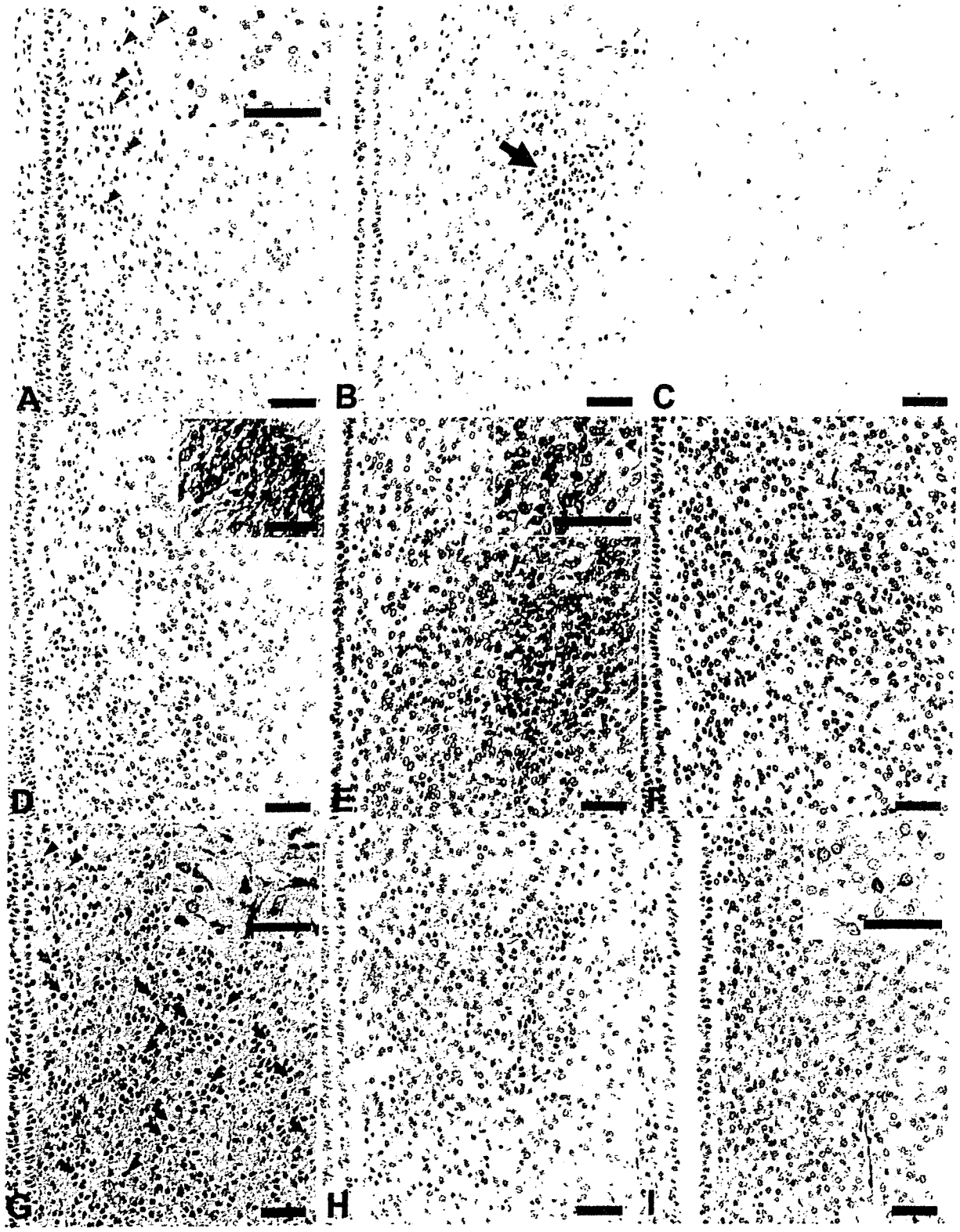

Figure 6

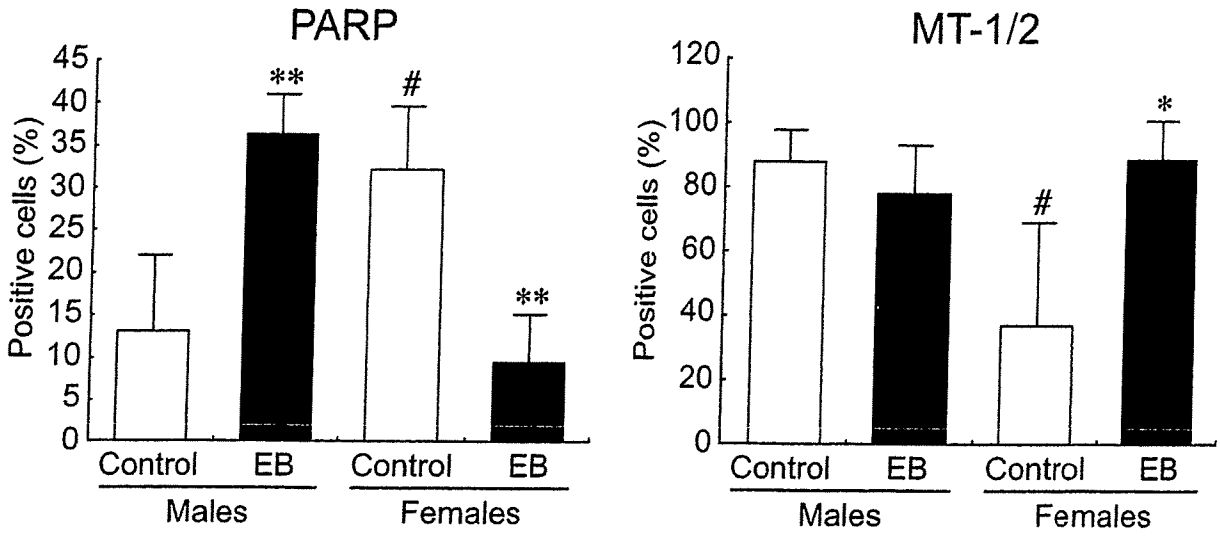

Figure 7 Nuclear immunoreactive cell percentages for PARP and MT-1/2 in neonatal rat MPOAs at PND 2. Significantly different from the corresponding controls ($^{*}p < 0.05$, $^{**}p < 0.01$). Significantly different from the male controls ($^{\#}p < 0.05$).

sponsible for subsequent sexually dimorphic development of this nucleus first occurs between PNDs seven and 10 (Davis et al., 1996), the number of genes exhibiting male-biased constitutive expression was much higher than in females at time points as early as PND 2 in the present study. This sex difference is presumably the reflection of growth and/or antiapoptotic effects for male-type large SDN under the influence of estradiol generated by aromatase from testosterone perinatally secreted from the developing testis (Matsumoto et al., 2000). Regarding responses to chemicals, the number of genes showing altered expression by EB or FA was far greater in females than in males, suggesting an effect on normal female sexual differentiation. Moreover, approximately 60% of genes showing male or female-biased expression demonstrated altered levels with EB in females, pointing to an involvement of genes necessary for normal processes of male- or female-type brain sexual differentiation in its disruptive effects. It is well known that the perinatal/neonatal treatment of animals with estrogenic compounds can affect sexual development of both sexes, resulting in reproductive dysfunction (Nagao et al., 1999; Odum et al., 2002; Tsukahara et al., 2003; Shibutani et al., 2005). With regard to the effects of antiandrogens, disruption of sexual development has generally been apparent in males, but the situation is largely unclear for females (Gray and Kelce, 1996; Wolf et al., 2004). With FA, however, prenatal exposure affects the volume of the anteroventral periventricular nucleus (AVPVN) in female rats (Lund et al., 2000) and the female sexual behavior in guinea pigs (Thornton et al., 1991). In addition, FA exerts antiprogestin activity (Chandrasekhar and Armstrong, 1989; Dukes et al., 2000).

Our search for genes showing altered expression by EB or FA revealed a total of four female-predominant genes with change by EB in both sexes, all up-regulated in males and down-regulated in females. Two of them are long interspersed repetitive DNAs, L1, or LINE, a class of mobile genetic elements named retrotransposons which can be amplified by retroposition, i.e. by a mechanism similar to that observed with retroviruses (Servomaa and Rytoamaa,

Table 6 Immunoreactivity of Protein Signals in the MPOA of Neonatal Rats Treated with EB[a]

	Males		Females	
Antigen	Control	EB	Control	EB
Number of animals	4	4	4	4
GluR1 (±/+)[b]	2[c](2/0)[d]	3(3/0)	4(3/1)	3(3/0)
GluR5 (present)	0	0	0	0
GluR6/7 (±/+/++)[b]	4(2/2/0)	4(0/4/0)	4(0/3/1)	4(2/2/0)
MAP2 (±/+/++)[b]	4(0/3/1)	4(0/3/1)	4(2/2/0)	4(2/2/0)

Protein signals with immunoexpression patterns for which morphometric analysis could not be applied were analyzed by visual estimation of the grade of intensity of immunoreactivity in the MPOA. MPOA, medial preoptic area; EB, estradiol benzoate; GluR1, glutamate receptor 1; GluR5, glutamate receptor 5; GluR6/7; glutamate receptor 6/7; MAP2, microtubule-associated protein 2.

[a] Rat neonates treated with EB at 10 μg/pup or vehicle on PND1 and sacrificed 24 h later were examined.

[b] Grades of intensity of immunoreactivity: ±, minimal; +, slight; ++, moderate; and +++, prominent.

[c] Total number of animals showing positive immunoreactivity.

[d] Number of animals with each grade.

1990). This group of retrotransposons includes regulatory signals and encodes two proteins, a RNA-binding protein and an integrase-replicase (Han and Boeke, 2005). The human genome contains about 500,000 LINES, accounting for roughly 17% of the total (Haoudi et al., 2004). Various environmental factors, such as steroid hormone-like agents and stressors can facilitate L1 transcription to alter cellular functions (Servomaa and Rytoamaa, 1990; Morales et al., 2002, 2003). Moreover, a regulatory role of L1 repeats at the promoter region has been reported with estrogen-related gene transcription (Hardy et al., 2001). During neuronal differentiation, retrotransposition events can alter the expression of neuronal genes, which, in turn, can influence neuronal cell fate (Muotri et al., 2005). Thus, the sex differences in the retrotransposon expression in the developing MPOA apparent here suggest roles in sex-dependent gene expression control, and alteration in their expression status due to EB may indicate roles as upstream regulators of genes necessary for brain sexual differentiation.

Two other genes showing up-regulation in males and down-regulation in females with EB, as well as female-biased expression, were *adprtl* and *NonO/p54nrb*. *Adprtl* encodes PARP-1, an abundant nuclear enzyme that is activated primarily by DNA damage; however, its excessive activation can lead to cell death (Skaper, 2003; Koh et al., 2005). Interestingly, sex differences exist regarding PARP-1 activation as well as nitric oxide toxicity in a mouse ischemic neurotoxicity model (McCullough et al., 2005). In the periventricular cell populations, poly(ADP-ribosyl)ation is basally activated by DNA strand breaks reflecting glutamate-nitric oxide neurotransmission (Pieper et al., 2000). In the present study, the measured level of PARP-immunoexpression at the SDN region was in line with the microarray data, suggesting an induction of subsequent programmed cell death in the female SDN-POA (Davis et al., 1996). Similarly, increased expression of PARP in males and its decrease in females with EB here may be linked to the decreased SDN volume in males in later life (Shibutani et al., 2005) and the decreased apoptosis in the female SDN after EB injection (Arai et al., 1996), respectively. NonO/p54nrb has been implicated in a variety of nuclear processes (Proteau et al., 2005). Indeed, this protein is known to act as a transcription factor necessary for adrenocortical steroidogenesis (Sewer et al., 2002), and as a transcriptional co-activator of the human androgen receptor (AR; Ishitani et al., 2003).

In the present study, a total of 15 genes exhibited altered expression due to FA in either sex, in addition to alteration by EB. Among them, 10 genes also exhibited sex differences in expression including the two genes for retrotransposons mentioned earlier. Interestingly, many of the 15 genes exhibited similar expression patterns with EB and FA, most being down-regulated in females, suggesting a common mechanism of action of the two chemicals. The following seven genes showed this particular expression pattern, in addition to the L1 repeat mentioned earlier: *PTPRF*/leukocyte common antigen-related (LAR) protein, *dlk*, two kinds of glutamate receptors, *dyskerin*, *MAP2*, and *efp*. In males, neonatal estrogen treatment affects the developing testis to suppress androgen secretion, presumably resulting in effects similar to antiandrogenicity on postnatal development (Atanassova et al., 1999). On the other hand, FA in the 20-day pubertal female assay using rats has been shown to exert ER-agonist activity on female sexual development, attributed to an imbalance between endogenous estrogenic and androgenic stimuli in the target organs (Kim et al., 2002).

Regarding glutamate receptors, mRNA expression of GluR1, the AMPA subtype found here with altered expression, is up-regulated in the AVPVN by estrogen in ovariectomized juvenile female rats (Gu et al., 1999). Hypothalamic GluR1 protein level was also increased in gonadectomized and estrogen-treated adult rats irrespective of the sex (Diano et al., 1997). Different from our female neonates, these results suggest that estrogen could up-regulate GluR1 levels in the juvenile/adult rat hypothalamus, probably through a different mechanism from that during sexual differentiation. In the female MPOA, we here could detect a slight, but nonsignificant increase in GluR1-immunoreactive cases when compared with those in males. Although we could not examine immunohistochemical localization of KA1 subunit here, other kainate receptor subtypes (GluR5, 6, and 7) have shown, in a study using adult rats, to be expressed in tanycytes, astrocytes, and neurons of the arcuate nucleus, with co-expression of AR or ER found in neurons in males and females, respectively (Diano et al., 1998). However, we could not detect any sex difference or EB-induced effect on the immunoreactivity of GluR5 or GluR6/7 in the neonatal MPOA.

PTPRF/LAR is a widely expressed tyrosine phosphatase that has been implicated in the regulation of a diverse range of signaling pathways, such as in the development and maintenance of excitatory synapses, and interestingly, disruption of its function results in reduction of surface AMPA receptors (Mooney and LeVea, 2003; Dunah et al., 2005). In the present study, AMPA subtype GluR1, as mentioned earlier, showed similar responses to EB and FA as well as a sex differ-

ence in mRNA expression, suggesting a coordinated action of PTPRF/LAR and AMPA receptors during brain sexual differentiation and its disruption.

MAP2 contributes to regulation of cytoskeletal organization and dynamics, and is expressed mainly in dendritic processes of neurons (Maccioni and Cambiazo, 1995). Posttranscriptional control of MAP2 expression has been reported in the female rat hippocampus in response to estrogen treatment or during the estrous cycle (Reyna-Neyra et al., 2002, 2004). Interestingly, estrogen can induce dendrite spines in the developing rat POA through activation of AMPA-kainate receptors by glutamate that may originate from astrocytes (Amateau and McCarthy, 2002). Inconsistent with the microarray data, MAP2-immunoreactivity in the neonatal MPOA here lacked any sex difference or change in expression on chemical treatment as in the case with above-mentioned GluR5 and GluR6/7.

Efp, a target gene product of ERα, is a RING-finger-dependent ubiquitin ligase that targets proteolysis of 14-3-3σ, a negative cell cycle regulator that causes G2 arrest (Urano et al., 2002), and is considered essential for estrogen-dependent tumor cell proliferation (Horie et al., 2003). This gene product is distributed mainly in estrogen-sensitive organs/tissues associated with ER co-expression (Orimo et al., 1995; Shimada et al., 2004). Dlk is a nuclear serine/threonine-specific kinase that has been implicated in the regulation of apoptosis by relocation to the cytoplasm, but its nuclear location has been suggestive of the roles for mitosis and cytokinesis (Preuss et al., 2003). Dyskerin, a nucleolar protein that modifies specific uridine residues of rRNA, also acting as a component of the telomerase complex, is a target molecule for skin and bone marrow failure syndrome called dyskeratosis congenita in human (Marrone et al., 2005). Dyskerin transcripts distribute ubiquitously in embryo-fetal tissues with notably high levels in epithelial and neural tissues (Heiss et al., 2000).

As a unique gene showing male-biased expression and increase with EB in females and decrease with FA in males, *MT1a* is of interest. MTs are considered to be important metal-binding proteins active in defense against heavy metal toxicity (Sogawa et al., 2001), and four major MT isoforms have so far been identified. In the present study, judging from the sequence information (accession no. AI176456) for the MT probes, either MT1 or 2 was suggested to be responsible for the particular expression pattern. Sex steroid-related expression changes in MT1 and/or 2 have been reported in the liver or brain of mice (Sogawa et al., 2001; Beltramini et al., 2004). In the brain, MT1 and 2 are expressed mainly in nonneuronal cells (Suzuki et al., 1994; Hidalgo et al., 2001), but certain levels are also found in neurons (Xie et al., 2004); as well as cytoplasmic expression, nuclear localization of MT has been reported in developing brain (Suzuki et al., 1994). Interestingly, kainic acid treatment can selectively induce MT1 in neurons and MT2 in glial cells in rats (Kim et al., 2003). Although the immunoreactivity of MT-1/2 was rather weak when compared with other brain areas and a nuclear expression was predominant in the neonatal MPOA here, male predominance may reflect a neuroprotective function, and expression changes due to EB and FA could indicate alteration in the regional hormonal environment in response to treatment.

In summary, we here established the basis for a global gene expression profiling method using paraffin-embedded, histologically defined small tissue areas with methacarn as a fixative. A male predominance in the number of genes showing constitutively higher expression suggestive of sex steroidal effects on the neonatal male MPOA was detected. Upon treatment with EB, many genes showing sex differences in expression demonstrated altered levels in females, in line with involvement of genes necessary for brain sexual differentiation in its disruption. Moreover, many genes commonly affected by EB and FA showed down-regulation in females with these drugs, suggesting common mechanisms shared between estrogenic and anti-androgenic chemicals in induction of endocrine center disruption in females, at least in early stages.

We thank Mrs. Keiko Kuroiwa for her technical assistance in conducting the immunohistochemical study. Dr. Lee was an Awardee of a Postdoctoral Fellowship from the Japan Society for the Promotion of Science during the performance of the study.

REFERENCES

Amateau SK, McCarthy MM. 2002. A novel mechanism of dendritic spine plasticity involving estradiol induction of prostaglandin-E_2. J Neurosci 22:8586–8596.

Arai Y, Sekine Y, Murakami S. 1996. Estrogen and apoptosis in the developing sexually dimorphic preoptic area in female rats. Neurosci Res 25:403–407.

Atanassova N, McKinnell C, Walker M, Turner KJ, Fisher JS, Morley M, Millar MR, et al. 1999. Permanent effects of neonatal estrogen exposure in rats on reproductive hormone levels, Sertoli cell number, and the efficiency of spermatogenesis in adulthood. Endocrinology 140:5364–5373.

Beltramini M, Zambenedetti P, Wittkowski W, Zatta P. 2004. Effects of steroid hormones on the Zn, Cu and MTI/II levels in the mouse brain. Brain Res 1013:134–141.

Chandrasekhar Y, Armstrong DT. 1989. Ability of progesterone to reverse anti-androgen (hydroxyflutamide)-induced interference with the preovulatory LH surge and ovulation in PMSG-primed immature rats. J Reprod Fertil 85:309–316.

Davis EC, Popper P, Gorski RA. 1996. The role of apoptosis in sexual differentiation of the rat sexually dimorphic nucleus of the preoptic area. Brain Res 734:10–18.

Diano S, Naftolin F, Horvath TL. 1997. Gonadal steroids target AMPA glutamate receptor-containing neurons in the rat hypothalamus, septum and amygdala: A morphological and biochemical study. Endocrinology 138:778–789.

Diano S, Naftolin F, Horvath TL. 1998. Kainate glutamate receptors (GluR5-7) in the rat arcuate nucleus: Relationship to tanycytes, astrocytes, neurons and gonadal steroid receptors. J Neuroendocrinol 10:239–247.

Dukes M, Furr BJ, Hughes LR, Tucker H, Woodburn JR. 2000. Nonsteroidal progestins and antiprogestins related to flutamide. Steroids 65:725–731.

Dunah AW, Hueske E, Wyszynski M, Hoogenraad CC, Jaworski J, Pak DT, Simonetta A, et al. 2005. LAR receptor protein tyrosine phosphatases in the development and maintenance of excitatory synapses. Nat Neurosci 8:458–467.

Gray LE Jr, Kelce WR. 1996. Latent effects of pesticides and toxic substances on sexual differentiation of rodents. Toxicol Ind Health 12:515–531.

Gu G, Varoqueaux F, Simerly RB. 1999. Hormonal regulation of glutamate receptor gene expression in the anteroventral periventricular nucleus of the hypothalamus. J Neurosci 19:3213–3222.

Han JS, Boeke JD. 2005. LINE-1 retrotransposons: Modulators of quantity and quality of mammalian gene expression? Bioessays 27:775–784.

Haoudi A, Semmes OJ, Mason JM, Cannon RE. 2004. Retrotransposition-competent human LINE-1 induces apoptosis in cancer cells with intact p53. J Biomed Biotechnol 2004:185–194.

Hardy DO, Niu EM, Catterall JF. 2001. Kap promoter analysis *in vivo*: A regulatory role for a truncated L1 repeat. Mol Cell Endocrinol 181:57–67.

Heiss NS, Bächner D, Salowsky R, Kolb A, Kioschis P, Poustka A. 2000. Gene structure and expression of the mouse dyskeratosis congenita gene, *dkc1*. Genomics 67: 153–163.

Hidalgo J, Aschner M, Zatta P, Vasak M. 2001. Roles of the metallothionein family of proteins in the central nervous system. Brain Res Bull 55:133–145.

Horie K, Urano T, Ikeda K, Inoue S. 2003. Estrogen-responsive RING finger protein controls breast cancer growth. J Steroid Biochem Mol Biol 85:101–104.

Ishitani K, Yoshida T, Kitagawa H, Ohta H, Nozawa S, Kato S. 2003. p54nrb acts as a transcriptional coactivator for activation function 1 of the human androgen receptor. Biochem Biophys Res Commun 306:660–665.

Kim D, Kim EH, Kim C, Sun W, Kim HJ, Uhm CS, Park SH, et al. 2003. Differential regulation of metallothionein-I, II, and III mRNA expression in the rat brain following kainic acid treatment. Neuroreport 14:679–682.

Kim HS, Shin JH, Moon HJ, Kim TS, Kang IH, Seok JH, Kim IY, et al. 2002. Evaluation of the 20-day pubertal female assay in Sprague-Dawley rats treated with DES, tamoxifen, testosterone, and flutamide. Toxicol Sci 67: 52–62.

Kocarek TA, Kraniak JM, Reddy AB. 1998. Regulation of rat hepatic cytochrome P450 expression by sterol biosynthesis inhibition: Inhibitors of squalene synthase are potent inducers of CYP2B expression in primary cultured rat hepatocytes and rat liver. Mol Pharmacol 54:474–484.

Koh DW, Dawson TM, Dawson VL. 2005. Poly(ADP-ribosyl)ation regulation of life and death in the nervous system. Cell Mol Life Sci 62:760–768.

Lund TD, Salyer DL, Fleming DE, Lephart ED. 2000. Pre or postnatal testosterone and flutamide effects on sexually dimorphic nuclei of the rat hypothalamus. Brain Res Dev Brain Res 120:261–266.

Maccioni RB, Cambiazo V. 1995. Role of microtubule-associated proteins in the control of microtubule assembly. Physiol Rev 75:835–864.

Marrone A, Walne A, Dokal I. 2005. Dyskeratosis congenita: Telomerase, telomeres and anticipation. Curr Opin Genet Dev 15:249–257.

Masutomi N, Shibutani M, Takagi H, Uneyama C, Takahashi N, Hirose M. 2003. Impact of dietary exposure to methoxychlor, genistein, or diisononyl phthalate during the perinatal period on the development of the rat endocrine/reproductive systems in later life. Toxicology 192: 149–170.

Matsumoto A, Sekine Y, Murakami S, Arai Y. 2000. Sexual differentiation of neuronal circuitry in the hypothalamus. In: Matsumoto A, editor. Sexual Differentiation of the Brain. Boca Raton: CRC Press, pp 203–227.

McCullough LD, Zeng Z, Blizzard KK, Debchoudhury I, Hurn PD. 2005. Ischemic nitric oxide and poly (ADP-ribose) polymerase-1 in cerebral ischemia: Male toxicity, female protection. J Cereb Blood Flow Metab 25:502–512.

McEwen BS, Alves SE. 1999. Estrogen actions in the central nervous system. Endocr Rev 20:279–307.

Meisel RL, Sachs BD. 1994. The physiology of male sexual behavior. In: Knobil E, Neills JD, editors. The Physiology of Reproduction, 2nd ed. New York: Raven Press, pp 3–106.

Meredith JM, Bennett C, Scallet AC. 2001. A practical three-dimensional reconstruction method to measure the volume of the sexually-dimorphic central nucleus of the medial preoptic area (MPOC) of the rat hypothalamus. J Neurosci Methods 104:113–121.

Mooney RA, LeVea CM. 2003. The leukocyte common antigen-related protein LAR: Candidate PTP for inhibitory targeting. Curr Top Med Chem 3:809–819.

Morales JF, Snow ET, Murnane JP. 2002. Environmental factors affecting transcription of the human L1 retrotransposon. I. Steroid hormone-like agents. Mutagenesis 17:193–200.

Morales JF, Snow ET, Murnane JP. 2003. Environmental factors affecting transcription of the human L1 retrotransposon. II. Stressors. Mutagenesis 18:151–158.

Muotri AR, Chu VT, Marchetto MC, Deng W, Moran JV, Gage FH. 2005. Somatic mosaicism in neuronal precursor cells mediated by L1 retrotransposition. Nature 435:903–910.

Nagao T, Saito Y, Usumi K, Kuwagata M, Imai K. 1999. Reproductive function in rats exposed neonatally to bisphenol A and estradiol benzoate. Reprod Toxicol 13:303–311.

Numan M. 1994. Maternal behavior. In: Knobil E, Neills JD, editors. The Physiology of Reproduction, 2nd ed. New York: Raven Press, pp 221–302.

Odum J, Lefevre PA, Tinwell H, Van Miller JP, Joiner RL, Chapin RE, Wallis NY, et al. 2002. Comparison of the developmental and reproductive toxicity of diethylstilbestrol administered to rats *in utero*, lactationally, preweaning, or postweaning. Toxicol Sci 68:147–163.

Orikasa C, Kondo Y, Hayashi S, McEwen BS, Sakuma Y. 2002. Sexually dimorphic expression of estrogen receptor β in the anteroventral periventricular nucleus of the rat preoptic area: Implication in luteinizing hormone surge. Proc Natl Acad Sci USA 99:3306–3311.

Orimo A, Inoue S, Ikeda K, Noji S, Muramatsu M. 1995. Molecular cloning, structure, and expression of mouse estrogen-responsive finger protein Efp. Co-localization with estrogen receptor mRNA in target organs. J Biol Chem 270:24406–24413.

Pieper AA, Blackshaw S, Clements EE, Brat DJ, Krug DK, White AJ, Pinto-Garcia P, et al. 2000. Poly(ADP-ribosyl) ation basally activated by DNA strand breaks reflects glutamate-nitric oxide neurotransmission. Proc Natl Acad Sci USA 97:1845–1850.

Preuss U, Bierbaum H, Buchenau P, Scheidtmann KH. 2003. DAP-like kinase, a member of the death-associated protein kinase family, associates with centrosomes, centromers, and the contractile ring during mitosis. Eur J Cell Biol 82:447–459.

Proteau A, Blier S, Albert AL, Lavoie SB, Traish AM, Vincent M. 2005. The multifunctional nuclear protein p54nrb is multiphosphorylated in mitosis and interacts with the mitotic regulator Pin1. J Mol Biol 346:1163–1172.

Reyna-Neyra A, Arias C, Ferrera P, Morimoto S, Camacho-Arroyo I. 2004. Changes in the content and distribution of microtubule associated protein 2 in the hippocampus of the rat during the estrous cycle. J Neurobiol 60:473–480.

Reyna-Neyra A, Camacho-Arroyo I, Ferrera P, Arias C. 2002. Estradiol and progesterone modify microtubule associated protein 2 content in the rat hippocampus. Brain Res Bull 58:607–612.

Rhees RW, Shryne JE, Gorski RA. 1990a. Onset of the hormone-sensitive perinatal period for sexual differentiation of the sexually dimorphic nucleus of the preoptic area in female rats. J Neurobiol 21:781–786.

Rhees RW, Shryne JE, Gorski RA. 1990b. Termination of the hormone-sensitive period for differentiation of the sexually dimorphic nucleus of the preoptic area in male and female rats. Dev Brain Res 52:17–23.

Rivas A, Fisher JS, McKinnell C, Atanassova N, Sharpe RM. 2002. Induction of reproductive tract developmental abnormalities in the male rat by lowering androgen production or action in combination with a low dose of diethylstilbestrol: Evidence for importance of the androgen-estrogen balance. Endocrinology 143:4797–4808.

Servomaa K, Rytomaa T. 1990. UV light and ionizing radiations cause programmed death of rat chloroleukaemia cells by inducing retropositions of a mobile DNA element (L1Rn). Int J Radiat Biol 57:331–343.

Sewer MB, Nguyen VQ, Huang CJ, Tucker PW, Kagawa N, Waterman MR. 2002. Transcriptional activation of human CYP17 in H295R adrenocortical cells depends on complex formation among p54nrb/NonO, protein-associated splicing factor, and SF-1, a complex that also participates in repression of transcription. Endocrinology 143:1280–1290.

Shibutani M, Masutomi N, Uneyama C, Abe N, Takagi H, Lee KY, Hirose M. 2005. Down-regulation of GAT-1 mRNA expression in the microdissected hypothalamic medial preoptic area of rat offspring exposed maternally to ethinylestradiol. Toxicology 208:35–48.

Shibutani M, Uneyama C. 2002. Methacarn: A fixation tool for multipurpose genetic analysis from paraffin-embedded tissues. In: Conn M, editor. Methods in Enzymology, Vol. 356. New York: Academic Press, pp 114–125.

Shibutani M, Uneyama C, Miyazaki K, Toyoda K, Hirose M. 2000. Methacarn fixation: A novel tool for analysis of gene expressions in paraffin-embedded tissue specimens. Lab Invest 80:199–208.

Shimada N, Suzuki T, Inoue S, Kato K, Imatani A, Sekine H, Ohara S, et al. 2004. Systemic distribution of estrogen-responsive finger protein (Efp) in human tissues. Mol Cell Endocrinol 218:147–153.

Skaper SD. 2003. Poly(ADP-ribose) polymerase-1 in acute neuronal death and inflammation: A strategy for neuroprotection. Ann NY Acad Sci 993:217–228; discussion 287–288.

Sogawa N, Sogawa CA, Oda N, Fujioka T, Onodera K, Furuta H. 2001. The effects of ovariectomy and female sex hormones on hepatic metallothionein-I gene expression after injection of cadmium chloride in mice. Pharmacol Res 44:53–57.

Suzuki K, Nakajima K, Otaki N, Kimura M. 1994. Metallothionein in developing human brain. Biol Signals 3:188–192.

Takagi H, Shibutani M, Kato N, Fujita H, Lee KY, Takigami S, Mitsumori K, et al. 2004. Microdissected region-specific gene expression analysis with methacarn-fixed, paraffin-embedded tissues by real-time RT-PCR. J Histochem Cytochem 52:903–913.

Tena-Sempere M, Gonzalez LC, Pinilla L, Huhtaniemi I, Aguilar E. 2001. Neonatal imprinting and regulation of estrogen receptor α and β mRNA expression by estrogen in the pituitary and hypothalamus of the male rat. Neuroendocrinology 73:12–25.

Thornton JE, Irving S, Goy RW. 1991. Effects of prenatal antiandrogen treatment on masculinization and defeminization of Guinea pigs. Physiol Behav 50: 471–475.

ukahara S, Ezawa N, Yamanouchi K. 2003. Neonatal estrogen decreases neural density of the septum-midbrain central gray connection underlying the lordosis-inhibiting system in female rats. Neuroendocrinology 78:226–233.

ieyama C, Shibutani M, Masutomi N, Takagi H, Hirose M. 2002. Methacarn fixation for genomic DNA analysis in microdissected, paraffin-embedded tissue specimens. J Histochem Cytochem 50:1237–1245.

ano T, Saito T, Tsukui T, Fujita M, Hosoi T, Muramatsu M, Ouchi Y, et al. 2002. Efp targets 14-3-3σ for proteolysis and promotes breast tumour growth. Nature 417: 871–875.

Wolf CJ, LeBlanc GA, Gray LE Jr. 2004. Interactive effects of vinclozolin and testosterone propionate on pregnancy and sexual differentiation of the male and female SD rat. Toxicol Sci 78:135–143.

Xie T, Tong L, McCann UD, Yuan J, Becker KG, Mechan AO, Cheadle C, et al. 2004. Identification and characterization of metallothionein-1 and -2 gene expression in the context of (±)3, 4-methylenedioxymethamphetamine-induced toxicity to brain dopaminergic neurons. J Neurosci 24:7043–7050.

Available online at www.sciencedirect.com
ScienceDirect
ELSEVIER
Biochemical and Biophysical Research Communications 354 (2007) 396–402
BBRC
www.elsevier.com/locate/ybbrc

Identification of amino acid residues in the Ah receptor involved in ligand binding

Kenji Goryo [a], Ai Suzuki [b], Carlos A. Del Carpio [b], Kazuhiro Siizaki [c,1], Eisuke Kuriyama [a], Yoshinori Mikami [a], Koshi Kinoshita [a], Ken-ichi Yasumoto [a], Agneta Rannug [d], Akira Miyamoto [b], Yoshiaki Fujii-Kuriyama [a,2], Kazuhiro Sogawa [a,*]

[a] *Department of Biomolecular Science, Graduate School of Life Sciences, Tohoku University, Sendai 980-8578, Japan*
[b] *Department of Materials Chemistry, Graduate School of Engineering, Tohoku University, Aoba-yama 6-6-11-1302, Sendai 980-8579, Japan*
[c] *Molecular and Cellular Toxicology Section, Environmental Health Sciences Division, National Institute for Environmental Studies, Onogawa, Tsukuba 305-8506, Japan*
[d] *Institute of Environmental Medicine, Karolinska Institutet, SE-171 77 Stockholm, Sweden*

Received 19 December 2006
Available online 10 January 2007

Abstract

The Ah receptor (AhR) is a ligand-activated transcription factor. Five amino acids as candidate amino acids necessary for ligand binding within or near the ligand-binding domain were selected based on their evolutional conservation and their aromatic nature that could interact with xenobiotic ligands. These amino acids were changed to Ala, and the mutated AhRs were subjected to a test of their transactivation activity in HeLa cells. Mutation of Phe318 completely lost its activity whereas other mutations only weakly impaired activity. The Leu-substituted mutant, AhR(Phe318Leu), activated the luciferase activity to the level comparable to wild type in the cells treated with 3-methylcholanthrene (MC) but not at all with β-naphthoflavone (β-NF). Ligand-binding activity of mutants was examined with [^{3}H]MC *in vitro*. AhR(Phe318Ala) could not bind to [^{3}H]MC. [^{3}H]MC bound by AhR(Phe318Leu) was competed with unlabeled MC but not with β-NF. A structural model of the ligand-binding domain was constructed.

Keywords: Ah receptor; Computer modeling; Ligand binding; PAS domain; Xenobiotics

Administration of xenobiotics such as 2,3,7,8-tetrachlorodibenzo-*p*-dioxin (TCDD), 3- methylcholanthrene (MC), and β-naphthoflavone (β-NF) into experimental animals induces several drug-metabolizing enzymes such as CYP1A1 in the liver. These inducers act as ligands for the Ah receptor (AhR), and subsequently, the ligand-activated AhR activates transcription of genes encoding the enzymes [1]. Numerous environmental pollutants, agricultural chemicals, and drugs are known to serve as ligands for the AhR. Polyhalogenated aromatic hydrocarbons such as TCDD and coplanar polychlorinated biphenyls, polycyclic aromatic hydrocarbons such as 3-MC, benzo[a]pyrene and formylindolo[3,2-*b*]carbazoles, and flavonoids such as β-NF are representative potent ligands [1,2]. The most noticeable characteristic of the ligands is that they are organic molecules with planar aromatic rings. In resting cells, the AhR is associated with Hsp90 in the cytoplasm

Abbreviations: AhR, aryl hydrocarbon receptor; MC, 3-methylcholanthrene; β-NF, β-naphthoflavone; TCDD, 2,3,7,8-tetrachlorodibenzo-*p*-dioxin; YFP, yellow fluorescent protein.

* Corresponding author. Fax: +81 22 795 6594.
E-mail address: sogawa@mail.tains.tohoku.ac.jp (K. Sogawa).
[1] Present address: Division of Environmental Genetics, Frontier Science Innovation Centre, Osaka Prefecture University, 1-2 Gakuen-cho, Sakai-city, Osaka 599-8570, Japan.
[2] Present address: Solution Oriented Research for Science and Technology, Japan Science and Technology Corporation, Honchou 4-1-8 Kawaguchi 332-0012, Japan; Department of Molecular and Developmental Biology, Center for Tsukuba Advanced Research Alliance, University of Tsukuba, Tsukuba 305-8577, Japan.

0006-291X/$ - see front matter © 2007 Elsevier Inc. All rights reserved.
doi:10.1016/j.bbrc.2006.12.227

as a soluble receptor. Owing to their lipophilic nature, it is presumed that ligands enter into cells by simple diffusion, and bind to the AhR. Ligand-induced conformation change of the AhR is believed to cause exposure of its nuclear localization signal and succeeding nuclear translocation of the liganded AhR. In the nucleus, the AhR forms a heterodimer with the Ah receptor nuclear translocator (Arnt), and then the heterodimer binds to a specific enhancer termed XRE (DRE or AhRE) localized in the upstream region of target genes [1]. The AhR and Arnt belong to the basic HLH–PAS domain protein family. Vertebrate PAS domains were generally composed of two imperfect repeated regions of about 110 amino acids named PAS-A and PAS-B domains. PAS and HLH domains serve as domains for dimerization with partner PAS proteins. In addition to the dimerization function, some PAS domains contain small organic compounds such as heme, probably for its sensing function [3]. The PAS-B domain of the AhR has the function of binding xenobiotic ligands [4]. The AhR homolog is also distributed in invertebrate species. Interestingly, recent studies demonstrate that *Drosophila* AhR (spineless) and *Caenorhabditis elegans* AhR (AhR-1) have no activity to bind foreign or endogenous chemicals as ligands. Although the protein has no ligand-binding activity, these AhRs heterodimerize with Arnt, binding to the DNA of which sequence is the same as XRE, and activating transcription [5,6].

In this study, we identified amino acids that play a key role in ligand binding of the AhR by several site-directed mutagenesis experiments. Furthermore, a three-dimensional model of the ligand-binding domain was constructed, which demonstrated good agreement with the results of the mutagenesis experiments.

Materials and methods

Construction of plasmids. pBOSFlag-mAhR-HA was constructed as follows. Oligonucleotides, 5′-CCACCGCCCATGGACTACAAAGACG ATGACGATAAAGGCATGGGCTGCA and 5′-GCCCATGCCTTTA TCGTCATCGTCTTTGTAGTCCATGGGCGGTGGAGCT for Flag peptide were inserted into the *Sac*I and *Pst*I site of pBluescript II. Full-length mouse AhR cDNA was inserted into the *Hin*dIII site of the generated plasmid. Using the plasmid as a template, a fragment of Flag-mAhR-HA was generated by PCR using primers, 5′-CCACCGCC CATGGACTACAAAGACGATGACGATAAAGGCATGGGCTGCA (forward) and 5′-CTCGAGCTAGGCGTAGGTCGGGCACGTCGAG GTCGACACACTCTGCACCTTGCTTAGGAATGCC (reverse), and the fragment was inserted into the *Xba*I site of the pEFBOS vector. Expression plasmids for mutated AhRs were produced by site- directed mutagenesis using PCR. Construction of XRE_4-tkLuc was described previously [7]. Chimeric plasmids for pFlag-mAhR-YFP were constructed as follows. A DNA fragment containing the Flag-AhR part of pBOSFlag-mAhR-HA was amplified by PCR, digested by *Bam*HI and *Sal*I and inserted into the *Nhe*I and *Xho*I sites of pEYFPN1 (Clonetech). The resultant plasmid was digested with *Eco*RI and *Bam*HI, treated with Klenow fragment and self-ligated to make the sequence in-frame.

DNA transfection and Western blotting. HeLa cells were grown in MEM supplemented with 10% fetal bovine serum. DNA transfection into Hela cells (grown in a 60 mm dish) was carried out by the calcium phosphate method using 2 μg reporter plasmid XRE_4-tkLuc, 1 μg pBOSFlag-mAhR-HA, 1 μg pBOSmArnt, and 1 μg pBOSLacZ for internal control as described [7]. Western blotting was performed using whole cell extracts from COS-7 cells transfected with pBOSFlag-mAhR-HA or its AhR mutants and a monoclonal anti-HA antibody (Roche, 12CA5). Because of low expression levels of the overexpressed proteins in HeLa cells, HEK293T cells were used to compare the expression levels of various mutants of the AhR, and it was found that they were relatively evenly expressed (data not shown).

Fluorescence observation of cells. CHO-K1 cells were provided by the Cell Resource Center for Biomedical Research, Institute of Development, Aging and Cancer, Tohoku University. Cells grown on the cover glass were transfected with 0.25 μg AhR–YFP fusion plasmids using FuGENE6 transfection reagent (Roche). After incubation for 40 h, cells were treated with MC or β-NF at a given concentration for 2 or 4 h, respectively. Imaging was performed with an Olympus BX50 fluorescence microscope equipped with a filter set (Olympus U-MYFPHQ) and an Olympus DP70 digital camera.

In vitro binding assay. Cytosolic extracts (1 mg protein/ml) from COS-7 cells transfected with expression plasmids for AhRs were prepared as described [8] and [^{3}H]-labeled MC (1 μCi, 1.2 Ci/mmol, Moravek Biochemicals) was added to 450 μl of the extracts. The mixture was incubated at 4 °C for 2 h with or without unlabeled competitors, treated with dextran-coated charcoal and subjected to fractionation by 10–30% (v/v) glycerol gradient centrifugation at 50,000 rpm at 1 °C for 14 h.

Modeling the structure of PAS-B domain. The multiple alignment in the homology modeling procedure was performed based on the predicted and the observed secondary structures of the reference proteins, FixL [9], HERG [10], PHY3 [11,12], EC DOS [13], HIF-2α [14], and PAS kinase [15], while taking into consideration the sequence and structure conservation in their families. A homology model of the mAhR PAS-B domain was generated by means of the modeling module in Insight 2000 (Accelrys Inc.). The docking process was performed using the docking module of the Cerius^2 system (Accelrys Inc.).

Results

Transactivation activity of mutated AhR

Candidate amino acids for ligand recognition and binding were selected on the basis of the following two assumptions. (1) Amino acids are conserved among vertebrate species whose AhRs exhibit ligand-binding activity, but are not conserved in the *Drosophila* and *C. elegans* AhRs that are deficient in binding activity. (2) Interactions between ligands and amino acids include the stacking force between aromatic side chains and aromatic rings of ligands because all ligands have hydrophobic aromatic rings. There were a number of amino acids that satisfied the first criterion. Accordingly, the second criterion was placed on the amino acids. Selection of amino acids satisfying the two criteria revealed five aromatic amino acids within and near the PAS-B domain as shown in Fig. 1A. The amino acids were mutated to Ala, and the transactivation activity of the corresponding mutated AhR was assayed. As shown in Fig. 1B, activity decreased to the basal level in the presence of MC by mutation of Phe318 to Ala. This loss of activity was also seen with other inducers including TCDD and β-NF. Other mutations caused a slight decrease in the transactivation activity. The Phe318 was changed to other amino acids as shown in Fig. 1C, and the transactivation activity of the mutated AhRs was assayed. Substitution to aromatic amino acids, Tyr or Trp, showed an inducible luciferase activity by the stimulus of MC and β-NF,

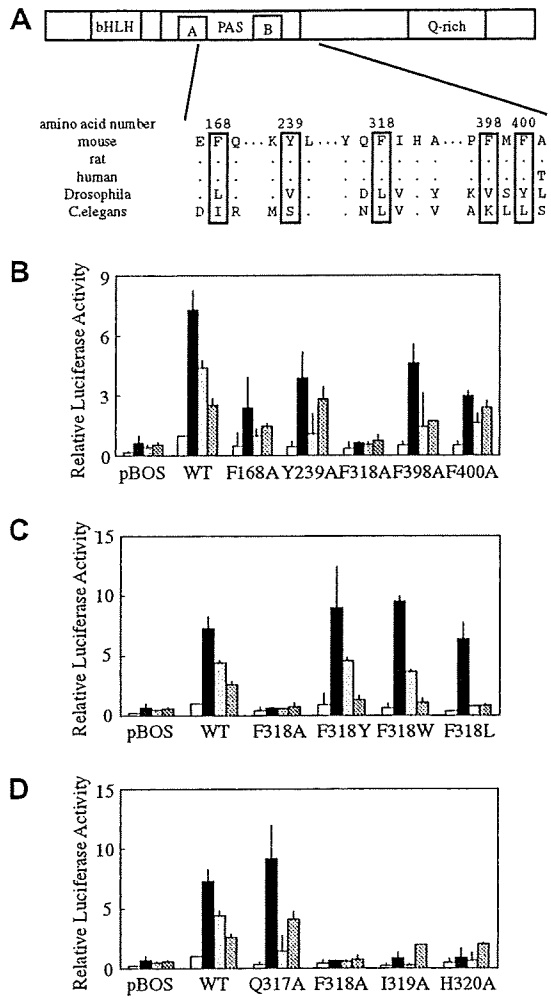

Fig. 1. Transactivation activity of the AhR and its mutants. (A) Alignment of the PAS-B sequences of vertebrate and invertebrate AhR. Structure of the mouse AhR is schematically shown above. Aromatic amino acid residues that were conserved within and around the PAS-B domain of mouse, human, and rat AhRs and that were not conserved in the domain of *Drosophila* and *C. elegans* AhRs were boxed. Dots indicate the same amino acids as those of the mouse AhR. (B) Transactivation activity of the AhRs with mutation of selected amino acids shown in (A). Selected aromatic amino acids were mutated to Ala, and cotransfected into HeLa cells with a reporter plasmid. Four hours after transfection, MC (1 μM), β-NF (0.5 μM), or TCDD (10 nM) were added to the culture medium and cells were further incubated for 40 h. Luciferase activity driven by the AhRs is shown. The values represent means ± SD of at least three separate determinations, and were normalized using the value(s) of wild type AhR treated with DMSO. Open bars, DMSO (vehicle); filled bars, MC; light gray bars, β-NF; dark gray bars, TCDD. (C,D) Transactivation activity of the AhRs with mutations of Phe318 to Ala, Tyr, Trp, and Leu, and transactivation activity of the AhRs with mutation of amino acids neighboring Phe318. Experimental procedures are shown in (B).

probably because the aromatic nature of the side chain was preserved, although induction by TCDD was weak. Mutation to Leu showed a luciferase activity in response to MC with an induction ratio similar to that of wild type, although induced activity was somewhat lower than that of wild type. Interestingly, this mutant exhibited no induction of luciferase activity by the addition of β-NF or TCDD, indicating that this mutation caused a ligand-binding specificity different from the wild type and suggesting that Phe318 may have contact with ligands. Three amino acid residues neighboring Phe318 were changed to Ala. The mutation of Gln317 had no effect on activity although induction by β-NF was weak (Fig. 1D). The mutation of Ile319 or His320 resulted in complete loss of activity, suggesting that these two amino acids also play an important role for ligand binding.

Nuclear translocation of AhRs in response to inducers

Chimeric proteins of mutated AhRs fused to YFP were expressed in CHO-K1 cells, and subcellular localization of the chimeric proteins was observed. These chimeric proteins were evenly expressed and showed transactivation activity similar to the AhR without YFP tag (data not shown). Fluorescence from the YFP moiety of the wild-type AhR fusion protein was diffused over the cell, and treatment of cells with MC caused accumulation of the signal in the nucleus as shown in Fig. 2. Approximately 50% of the fluorescent cells showed nuclear localization at the maximal concentration of MC. The nuclear accumulation was accomplished within 2 h and dependent on the concentration of MC. Nuclear translocation was also observed by the addition of β-NF, although the rate of the translocation was slow, and 4 h was required for completion. The reason is not clear as to why nuclear localization of expressed AhR–YFP did not occur in all fluorescent cells even at high concentrations of inducers. Nuclear localization of mutant AhR(Phe318Ala) was similarly examined. When neither MC nor β-NF was added, nuclear accumulation of the mutant did not occur. Mutant AhR(Phe318Leu) was translocated into the nucleus by the addition of MC similar to the level of the wild type. However, the mutant remained in the cytosol with the addition of β-NF, in accordance with the result of transactivation activity of the mutant. Taken together, these results strongly suggest that stimulus-dependent nuclear localization of mutated AhRs is the causal event for their transactivation activity.

Ligand-binding activity of mutated AhRs

In vitro binding activity of mutated AhRs to [^{3}H]-labeled MC was examined using cytosolic extracts of COS-7 cells transfected with expression plasmids for the AhRs. A clear peak at around the 9S position of the [^{3}H]MC-AhR complex appeared in the glycerol gradient as shown in Fig. 3A. This binding of the radioactive ligand was competed out with 22 times the molar excess of unlabeled MC or β-NF. A similar binding signal was also observed when cytosol containing AhR(Phe318Leu) was used. This signal was competed with unlabeled MC. However, unlabeled β-NF could not compete with the [^{3}H]MC bound to the mutated AhR, reflecting the results of transactivation and

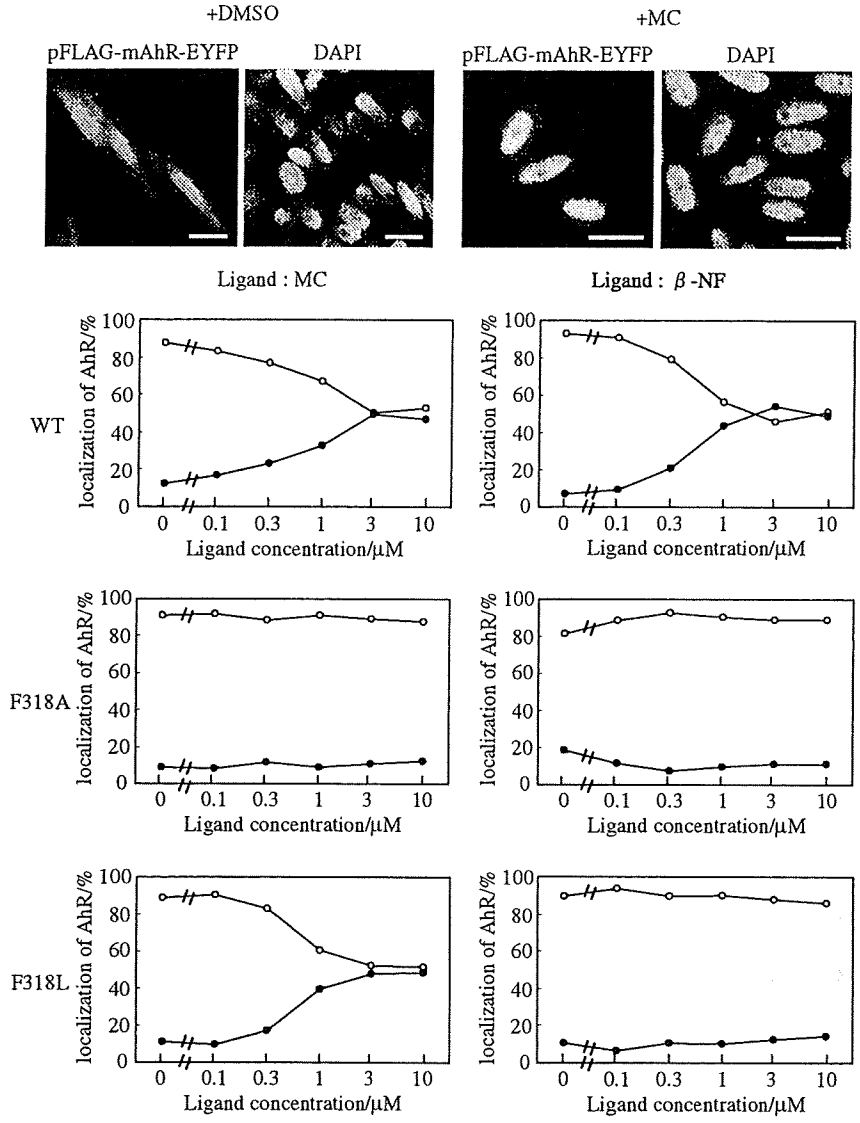

Fig. 2. Nuclear translocation of the AhR and its mutants. CHO-K1 cells were transfected with AhR–YFP-fusion plasmids, and treated with inducers for 2 h (MC) or 4 h (β-NF) before fixation in 4% paraformaldehyde. The fixed cells were counterstained with DAPI. Typical images of fluorescent cells after treatment with DMSO (vehicle) and MC are shown above. Scale bars, 20 μm. Approximately 300 cells were randomly selected, and percentages of cells with only nuclear localization (shown by closed circles) and cells with both nuclear and cytosolic localization (shown by open circles) of the chimeric protein are shown.

nuclear translocation experiments. When cytosol fraction containing expressed AhR(Phe318Ala) was used, no signal of ligand binding was detected. The mutated AhRs were evenly expressed in COS-7 cells as shown in Fig. 3B.

Modeling the AhR ligand-binding domain

Since the three-dimensional (3D) structure of AhR has not been elucidated so far, and previously reported 3D models of the ligand-binding domain have failed to identify Phe318 as a ligand-recognition amino acid [16], we concentrated on the active site of AhR, and obtained a 3D model for it using comparative modeling techniques. A combined FASTA and PSI-BLAST search of the protein data bank (PDB) [17] reveals a high number of matches between mouse AhR PAS-B and other PAS proteins, including HLF (HIF-2α), several histidine kinases, and other light receptors as well as sensor proteins (oxygen/redox sensors) and ion channels (data not shown). Sequences such as HLF, PHY3, HERG, FixL, EC Dos, and PAS kinase were found that were based on a moderate sequence similarity, characterized by E values of less than 10^{-3}. Fig. 4A illustrates the multiple sequence alignment of AhR PAS-B with these sequences. A further alignment of the secondary structure predicted for AhR PAS-B and the secondary structures for the 3D structures extracted from PDB

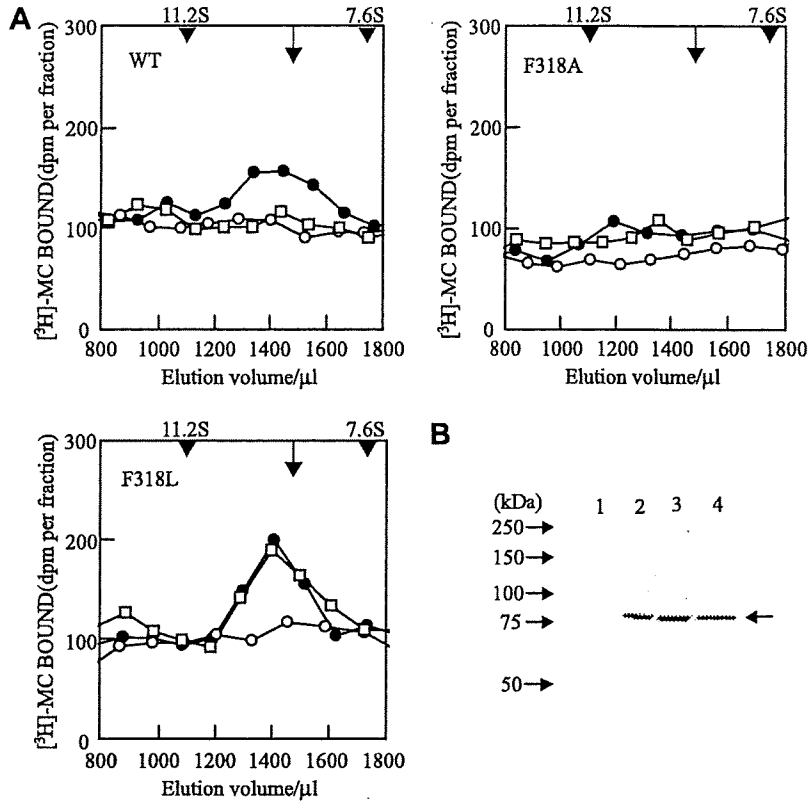

Fig. 3. Ligand-binding activity of the AhR and its mutants. (A) Binding of mutant AhRs to [^{3}H]-labeled MC. AhRs were expressed in COS-7 cells and cytosolic extracts were prepared. Glycerol gradient centrifugation was performed as described under Materials and methods. Fractions (about 100 μl) were collected and radioactivity was counted on a liquid scintillation counter. Catalase (11.2S) and fibrinogen (7.6S) were used as size markers. Arrows show the position of 9S. Filled circle, [^{3}H]MC with DMSO; open circle, [^{3}H]MC with unlabeled MC; open square, [^{3}H]MC with unlabeled β-NF. (B) Expression of mutant AhRs. Western blotting analysis using 20 μg of cell extracts was performed by the ECL plus Western blotting detection system kit. Lane 1, whole cell extracts without transfection; lanes 2–4, cytosolic extracts of cells transfected with expression plasmid for AhR, AhR(Phe318Ala), and AhR(Phe318Leu), respectively. An arrow shows the bands of the AhR.

indicate that the fold of HLF is the optimal template on which to model AhR PAS-B (Fig. 4B). The threading process of the AhR sequence into the template was performed using Swiss PDB viewer (spdbv) software. The structure was further minimized using the GROMOS force field embedded in spdbv to optimize the position of the lateral chains of the amino acids constituting the receptor.

Assisted by the docking module in Cerius^2, we first mapped plausible ligand-binding pockets for the model of AhR PAS-B. A unique deep cavity was recognized by the system, the boundaries of which are constituted by the amino acids in Table 1. The model was then used to dock three ligand molecules, MC, β-NF, and TCDD. The docking process was also performed using the Cerius^2 software. Orientations for the ligands within the binding pocket ranked as the highest by the docking software were further minimized so as to obtain reliable 3D structures for the receptor–ligand complexes. Amino acids in contact with the ligand are identified by computing the fraction of SASA (solvent accessible surface area) buried by each of the amino acids on the ligand. We performed this calculation for β-NF, and Table 1 illustrates the decrement in SASA of β-NF when docked to the cavity of the model of AhR by each of the amino acids composing the cavity. The SASA is computed using Richards' algorithm [18], and a radius for the solvent molecule (water) of 1.4 Å. The buried SASA is calculated as the difference of the SASA of β-NF at the isolated state minus the SASA of β-NF when it is in contact with each of the amino acids listed in Table 1. Docking models of the complex of AhR with TCDD, MC or β-NF, show their extensive contact with Phe318, Ile319, and His320 (Fig. 4C). Extensive hydrophobic interaction can also be observed with Ala328, Met342, Leu347, and Leu348. Two lysine residues (Lys284 and Lys286) suggest the formation of hydrogen bonds with the oxygens on the aromatic rings of β-NF.

Discussion

From the results shown in Fig. 1, it is suggested that Phe318 plays a critical role in ligand binding to AhR. The importance of this amino acid is also demonstrated by the complex model of AhR PAS-B that we built by comparative modeling and docking simulations. The decrement

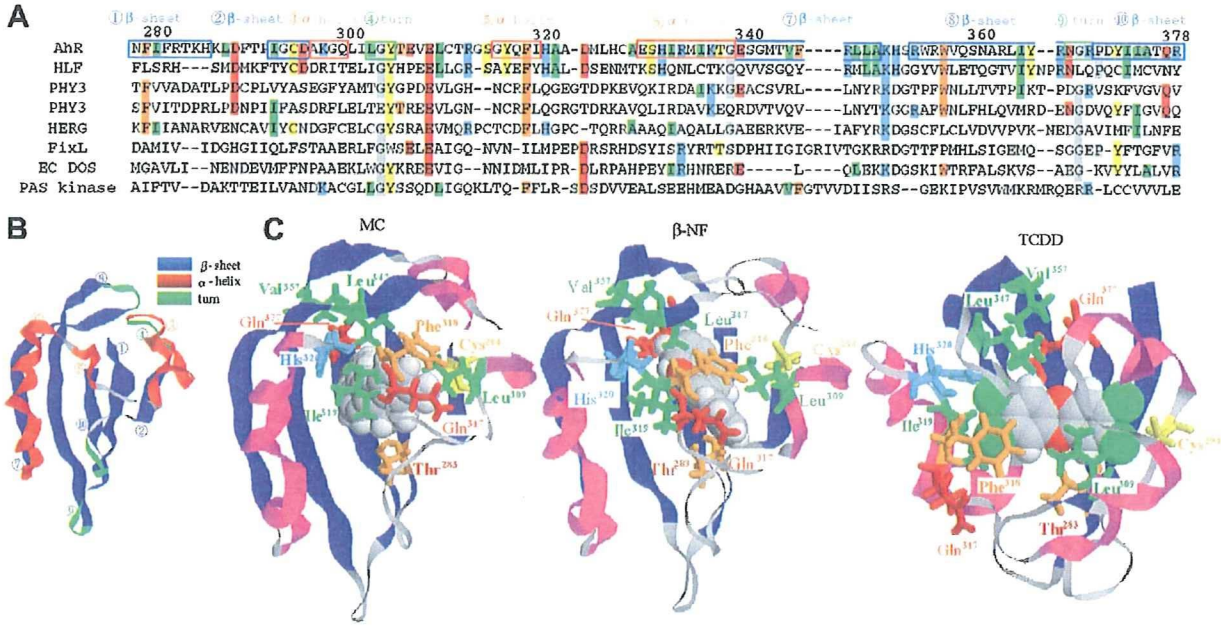

Fig. 4. Model of the AhR PAS-B domain and contacts between ligands and amino acid residues in the binding pocket. (A) Sequence alignment of AhR-related sequences. Sequences of Mouse AhR, human HLF (HIF-2α), PHY3 from *Chlamydomonas reinhardtii* (upper sequence) and *Adiantum capillus-veneris* (lower sequence), human HERG, *Bradyrhizobium japonicus* FixL, *Escherichia coli* EC DOS and human PAS kinase were aligned. Secondary structure regions are shown above the sequences. (B) Ribbon-style drawing of the AhR PAS-B domain. Numbers show the secondary structure regions as shown in (A). (C) Model of MC, β-NF, and TCDD in the binding site of AhR PAS-B domain. Secondary structure elements are colored blue (strands) and red (helices).

Table 1
Calculated buried SASA of β-NF by amino acids in the binding region of AhR

Amino acid	Difference in SASA (in Å^2) for β-NF
THR283	0.07
LYS284	73.37
LYS286	49.73
CYS294	0.07
GLN299	72.54
GLY303	47.77
TYR304	29.22
LEU309	0.07
CYS310	27.07
GLY315	46.93
GLN317	0.07
PHE318	84.37
ILE319	77.81
HIS320	60.62
ALA328	81.26
SER330	43.35
MET342	73.18
LEU347	88.59
LEU348	87.90
ALA349	42.20
VAL357	37.66
SER359	61.20
ALA375	0.00
GLN377	41.40

in the SASA of β-NF due to contact with Phe318 is large (about 84 Å^2, Table 1), suggesting that extensive interaction exists between the residue and the ligand. Mutation of Phe318 by Leu completely eliminated responsiveness of the mutant towards β-NF, although responsiveness to MC remained unchanged. Binding experiments using [^{3}H]MC corroborate the geometry of our modeled complex, since the location of Phe318 at the ligand-binding surface of the receptor plays a key role in ligand-binding specificity. This is clearly shown by the mutations performed on Phe318 that caused changes in the binding activity of the receptor. Moreover, two amino acids, Ile319 and His320, neighboring Phe318, were both found to play an essential role in the binding activity of the receptor. Although contact surface areas of these amino acids with the docked ligands are less than that of Phe318, their relevance in the binding affinity of the receptor cannot be neglected. In fact, Ile319 has been reported to be important in avian AhRs [19]. The Ile residue (Ile324 corresponding to Ile319 in the mouse AhR) of the chicken AhR that showed high affinity towards TCDD was changed to Val in tern AhR that exhibited low TCDD-binding activity. As shown in Fig. 1D, a large decrement in the activity of the receptor was observed when they were mutated to Ala. Therefore, the importance of these two amino acids in the binding of the ligands can be rationalized in terms of their bulky lateral chains and polar characteristics. The imidazole group in His confers it a polar property absent in Ala while Ile has a larger chain and is more strongly hydrophobic. Thus, mutations of these amino acids have strong repercussions in the activity of the receptor. Ala375, whose allelic mutation was demonstrated to be

responsible for the different ligand-binding affinity between C57BL/6 and DBA/2 mouse strains [8] was also exposed into the ligand-binding pocket, although it does not appear to be in direct contact with β-NF in the model. Further mutagenesis studies are necessary to confirm the amino acids composing ligand-binding domain of the AhR.

Acknowledgments

This work was supported in part by Grant-in-Aid for research from the Ministry of Education, Culture, Sports, Science and Technology of Japan, and by funds for Research for the Future Program of JSPS.

References

[1] J. Mimura, Y. Fujii-Kuriyama, Molecular mechanisms of AhR functions in the regulation of cytochrome P450 genes, Biochem. Biophys. Res. Commun. 338 (2005) 311–317.

[2] L. Bergander, N. Wahlstrom, T. Alsberg, J. Bergman, A. Rannug, U. Rannug, Characterization of in vitro metabolites of the aryl hydrocarbon receptor ligand 6-formylindolo[3,2-*b*]carbazole by liquid chromatography-mass spectrometry and NMR, Drug Metab. Dispos. 31 (2003) 233–241.

[3] E.M. Dioum, J. Rutter, J.R. Tuckerman, G. Gonzalez, M.A. Gilles-Gonzalez, S.L. Mcknight, NPAS2: a gas-responsive transcription factor, Science 298 (2002) 2385–2387.

[4] K.M. Dolwick, H.I. Swanson, C.A. Bradfield, In vitro analysis of Ah receptor domains involved in ligand-activated DNA recognition, Proc. Natl. Acad. Sci. USA 90 (1993) 8566–8570.

[5] J.A. Powell-Coffman, C.A. Bradfield, W.B. Wood, *Caenorhabditis elegans* orthologs of the aryl hydrocarbon receptor and its heterodimerization partner the aryl hydrocarbon receptor nuclear translocator, Proc. Natl. Acad. Sci. USA 95 (1998) 2844–2849.

[6] R.B. Emmons, D. Duncan, P.A. Estes, P. Kiefel, J.T. Mosher, M. Sonnenfeld, M.P. Ward, I. Duncan, S.T. Crews, The spineless-aristapedia and tango bHLH-PAS proteins interact to control antennal and tarsal development in *Drosophila*, Development 126 (1999) 3937–3945.

[7] J. Mimura, M. Ema, K. Sogawa, Y. Fujii-Kuriyama, Identification of a novel mechanism of regulation of Ah (dioxin) receptor function, Genes Dev. 13 (1999) 20–25.

[8] M. Ema, N. Ohe, M. Suzuki, J. Mimura, K. Sogawa, S. Ikawa, Y. Fujii-Kuriyama, Dioxin binding activities of polymorphic forms of mouse and human arylhydrocarbon receptors, J. Biol. Chem. 269 (1994) 27337–27343.

[9] W. Gong, B. Hao, S.S. Mansy, G. Gonzalez, M. Gilles-Gonzalez, M.K. Chan, Structure of a biological oxygen sensor: a new mechanism for heme-driven signal transduction, Proc. Natl. Acad. Sci. USA 95 (1998) 15177–15182.

[10] J.H.M. Cabral, A. Lee, S.L. Cohen, B.T. Chait, M. Li, R. Mackinnon, Crystal structure and functional analysis of the HERG potassium channel N terminus: a eukaryotic PAS domain, Cell 95 (1998) 649–655.

[11] S. Crosson, K. Moffat, Photoexcited structure of a plant photoreceptor domain reveals a light-driven molecular switch, Plant Cell 14 (2002) 1067–1075.

[12] T. Kinoshita, M. Doi, N. Suetsugu, T. Kagawa, M. Wada, K. Shimazaki, Phot1 and phot2 mediate blue light regulation of stomatal opening, Nature 414 (2001) 656–660.

[13] H. Kurokawa, D.S. Lee, M. Watanabe, I. Sagami, B. Mikami, C.S. Raman, T. Shimizu, A redox-controlled molecular switch revealed by the crystal structure of a bacterial heme PAS sensor, J. Biol. Chem. 279 (2004) 20186–201893.

[14] P.J. Erbel, P.B. Card, O. Karakuzu, R.K. Bruick, K.H. Gardner, Structural basis for PAS domain heterodimerization in the basic helix–loop–helix-PAS transcription factor hypoxia-inducible factor, Proc. Natl. Acad. Sci. USA 100 (2003) 15504–15509.

[15] J. Rutter, C.H. Michnoff, S.M. Harper, K.H. Gardner, S.L. McKnight, PAS kinase: an evolutionarily conserved PAS domain-regulated serine/threonine kinase, Proc. Natl. Acad. Sci. USA 98 (2001) 8991–8996.

[16] M. Procopio, A. Lahm, A. Tramontano, L. Bonati, D. Pitea, A model for recognition of polychlorinated dibenzo-*p*-dioxins by the aryl hydrocarbon receptor, Eur. J. Biochem. 269 (2002) 13–18.

[17] H.M. Berman, J. Westbrook, Z. Feng, G. Gilliland, T.N. Bhat, H. Weissig, I.N. Shindyalov, P.E. Bourne, The protein data bank, Nucleic Acids Res. 28 (2000) 235–242.

[18] B. Lee, F.M. Richards, Interaction of protein structures: estimation of static accessibility, J. Mol. Biol. 55 (1971) 379–400.

[19] S.I. Karchner, D.G. Franks, S.W. Kennedy, M.E. Hahn, The molecular basis for differential dioxin sensitivity in birds: role of the aryl hydrocarbon receptor, Proc. Natl. Acad. Sci. USA 103 (2006) 6252–6257.

Available online at www.sciencedirect.com
ScienceDirect
Reproductive Toxicology 24 (2007) 178–198
Reproductive Toxicology
www.elsevier.com/locate/reprotox

Review

In vitro molecular mechanisms of bisphenol A action☆

Yelena B. Wetherill[a,b], Benson T. Akingbemi[c], Jun Kanno[d], John A. McLachlan[e], Angel Nadal[f], Carlos Sonnenschein[g], Cheryl S. Watson[h], R. Thomas Zoeller[i], Scott M. Belcher[j,*]

[a] *Department of Environmental Health, Harvard School of Public Health, Boston, MA 02115, United States*
[b] *Department of Epidemiology, Harvard School of Public Health, Boston, MA 02115, United States*
[c] *Department of Anatomy, Physiology and Pharmacology, Auburn University, AL 36849, United States*
[d] *Division of Cellular and Molecular Toxicology, National Institute of Health Sciences, Tokyo 158-8501, Japan*
[e] *Department of Pharmacology and Environmental Endocrinology Lab, Center for Bioenvironmental Research, Tulane University, New Orleans, LA 70112, United States*
[f] *Instituto de Bioingeniería, Universidad Miguel Hernández de Elche, Elche 03202, Alicante, Spain*
[g] *Department of Anatomy and Cellular Biology, Tufts University School of Medicine, Boston, MA 02111, United States*
[h] *Biochemisty and Molecular Biology Department, University of Texas Medical Branch, Galveston, TX 77555, United States*
[i] *Laboratory of Molecular and Cellular Neurobiology, University of Massachusetts Amherst, MA 01003, United States*
[j] *University of Cincinnati College of Medicine, Department of Pharmacology and Cell Biophysics, Cincinnati, OH 45267, United States*

Received 12 April 2007; accepted 18 May 2007
Available online 29 May 2007

Abstract

Bisphenol A (BPA, 2,2-bis (4-hydroxyphenyl) propane; CAS# 80-05-7) is a chemical used primarily in the manufacture of polycarbonate plastic, epoxy resins and as a non-polymer additive to other plastics. Recent evidence has demonstrated that human and wildlife populations are exposed to levels of BPA which cause adverse reproductive and developmental effects in a number of different wildlife species and laboratory animal models. However, there are major uncertainties surrounding the spectrum of BPA's mechanisms of action, the tissue-specific impacts of exposures, and the critical windows of susceptibility during which target tissues are sensitive to BPA exposures. As a foundation to address some of those uncertainties, this review was prepared by the "*In vitro*" expert sub-panel assembled during the "*Bisphenol A: An Examination of the Relevance of Ecological, In vitro and Laboratory Animal Studies for Assessing Risks to Human Health*" workshop held in Chapel Hill, NC, Nov 28-29, 2006. The specific charge of this expert panel was to review and assess the strength of the published literature pertaining to the mechanisms of BPA action.

Abbreviations: 4-*tert*-OP, 4-tertiary octylphenol; 17α-EE, 17alpha-ethinyl estradiol; AR, androgen receptor; ARE, androgen response element; BADGE, bisphenol A diglycidyl ether; BFDGE, bisphenol F diglycidyl ether; BP-3, *p,p'*-dihydroxybenzphenone; BP-4, 2,2-bis(*m*-methyl-*p*-hydroxyphenyl)propane; BP-5, 2,2-bis(*p*-hydroxyphenyl) perfluoropropane; BPA, 2,2-bis(4-hydroxyphenyl) propane; BPA-OMe, 2,2-bis(4-methoxyphenyl)propane; BPE, 1,1-bis(4-hydroxyphenyl)ethane; BPF, 4,4'-methylenebisphenol; BPM, 4,4'-(1,3-phenylenedisopropylidene)bisphenol; BPP, 4,4'-(1,4-phenylenedisopropylidene)phenol; BPS, 4,4'-sulfonyldiphenol; BPZ, 4,4'-cyclohexylidenebisphenol; DDE, *o,p'*-dichlorodiphenylethylene; *o,p'*-DDT, 1,1,1-trichloro-2-[*o*-chlorophenyl]-2-[*p*-chlorophenyl]ethane; DEHP, bis(2-ethylhexyl)phthalate; DES, diethylstilbesterol; DHT, dihydrotestosterone; DMSO, dimethyl sulfoxide; E2, 17beta-estradiol; EDC, endocrine disrupting chemical; ELISA, enzyme-linked immunosorbent assay; ER, estrogen receptor; ERE, estrogen response element; ETOH, ethanol; GFAP, glial fibrillary acidic protein; GFP, green fluorescent protein; GH, growth hormone; HBSS, Hank's buffered saline solutions; h, hour; HRP, horseradish peroxidase; inos, inducible nitric oxide synthase; KLH, keyhole limpet hemocyanin; LPS, lipopolysaccharide; min, minute; NO, nitric oxide; NP, nonylphenol; OP, octylphenol; PCB, polychlorinated biphenyl; PMA, phorbol 12-myristate 13-acetate; PR, progesterone receptor; PSA, prostrate specific antigen; RIA, radio-immuno assay; RT-PCR, reverse transcription-polymerase chain reaction; RXR, retinoid X receptor; s, second; TCDD, 2,3,7,8-tetrachloro-dibenzo-*p*-dioxin; T3, L-3,3',5-triiodothyronine; T4, 3,3',5,5'-tetraiodo-L-thyronine; TR, thyroid hormone receptor.

☆ SMB is supported by the NIH grants RO1-ES015145 and the University of Cincinnati Center for Environmental Genetics (P30-ES06096). YBW is supported by the NIEHS Kirschstein-National Research Service Award (T32 ES07069-26).

* Corresponding author at: Department of Pharmacology and Cell Biophysics, University of Cincinnati College of Medicine, 231 Albert Sabin Way, P.O. Box 670575, Cincinnati, OH 45267-0575, Untied States. Tel.: +1 513 558 1721; fax: +1 513 558 4329.
E-mail address: scott.belcher@uc.edu (S.M. Belcher).

0890-6238/$ – see front matter © 2007 Published by Elsevier Inc.
doi:10.1016/j.reprotox.2007.05.010

The resulting document is a detailed review of published studies that have focused on the mechanistic basis of BPA action in diverse experimental models and an assessment of the strength of the evidence regarding the published BPA research.

Keywords: Bisphenol A (BPA, 2,2-bis(4-hydroxyphenyl) propane; Endocrine disruption; Endocrine disrupting chemical (EDC); Rapid signaling; Estrogen receptor; Androgen receptor; Thyroid receptor; Thyroid hormone; GPR30; Non-classical membrane estrogen receptor; Immune system; Allergic resonse; *In vitro* mechanisms; Cell specificity; Expert panel review

Contents

1. Introduction

Bisphenol A (BPA, 2,2-bis(4-hydroxyphenyl) propane; CAS# 80-05-7) is a chemical used primarily in the manufacture of polycarbonate plastic, epoxy resins and as a non-polymer additive to other plastics. Because of BPA's extensive use in the manufacture of consumer goods and products, including polycarbonate food containers and utensils, dental sealants, protective coatings, some flame retardants, and water supply pipes, there is a widespread and well-documented human exposure to BPA [1,2]. Recent discoveries regarding the environmental distribution and presence of BPA in humans and wildlife have generated persistent scientific, regulatory, and public interest in assessing the potential health risks associated with BPA exposure. The detection of adverse health effects in a number of laboratory animal models upon exposure to environmentally relevant doses of BPA, as well as potential effects on human reproduction and development, have fueled additional concern. While the exposure of wildlife species and humans to BPA has been increasingly reported in the literature, there are research gaps regarding its molecular mechanisms of action, the tissue-specific impacts of exposure, and knowledge of the critical windows of susceptibility, during which target tissues are especially sensitive to BPA.

The lack of an integrated and systemic understanding of BPA's endocrine disruptive actions has considerably complicated risk assessment efforts and safety recommendations by regulatory agencies. Current limitations in understanding the global consequences of BPA exposures include incomplete understanding of the cell/tissue specific actions and effects, a limited understanding of the receptor systems and signaling cascades through which BPA acts, and understanding when these receptors and signaling systems are present and active in target cells at different critical times of sensitivity during the entire life-span.

2. Overview

This white paper was prepared for the *in vitro* expert subpanel assembled during the "Bisphenol A: An Examination of the Relevance of Ecological, *In vitro* and Laboratory Animal Studies for Assessing Risks to Human Health" workshop at the NIEHS. The specific charge of this expert panel was to review and assess the strength of the published literature pertaining to the mechanisms of BPA action. Particular attention was paid to studies employing *in vitro* models and the results, findings and conclusions from those studies were integrated into the broader biological/physiologic context of BPA action. Thus, the goal of